

On the Innovative Design for Hybrid CVTs with Mechanical Reverse Driving Mode

Chun-Yao Yeh* and Hong-Sen Yan

Keywords : systematical design procedure, CVTs, mechanical reverse driving mode, hybrid transmission.

ABSTRACT

This paper aims to develop a systematical design procedure to synthesize all feasible hybrid transmissions, mainly on series-parallel hybrid continuous variable transmissions (CVTs) with a mechanical reverse driving mode. Following the proposed design procedure and subject to the design constraints, 21 novel hybrid CVTs are synthesized. One is shown that the transmission system makes possible a maximum vehicle speed of 226 km/h, a 0~100 km/h acceleration time of 7.1439 seconds, and a gradeability of 51.16 %. A simulation model is developed to investigate the fuel efficiency performance of the proposed design. In addition, a control strategy is constructed to dynamically adjust the operation mode of the hybrid transmission in accordance with changes in the road conditions. It is shown that the simulated vehicle with the proposed hybrid CVT achieves a fuel consumption of 45 mpg under urban driving cycles and 36 mpg under highway driving conditions. As such, the HEV performance is highly competitive with that of existing HEVs on the commercial market.

INTRODUCTION

In response to growing global environmental awareness and increasingly stringent international laws and regulations on vehicle emissions, the automotive industry has invested massive sums in the development of green vehicles over the past few decades. Although many electric vehicles have been developed, their commercialization is hindered by

existing battery technology, which necessitates their frequent recharging. Hybrid Electric Vehicles (HEVs) are a combination of conventional internal-combustion engine vehicles and electric vehicles. HEVs use two or more power sources to drive the vehicle. The engine provides most of the energy to meet the vehicle needs, while the motor serves mainly to increase the fuel efficiency by adjusting the speed and torque in such a way as to enable the engine to work in its optimum condition. As a result, HEVs combine the advantages of both conventional and electric vehicles, have attracted much interest in recent years. With their stable power, good acceleration performance, high fuel efficiency and lack of carbon emissions, HEVs are regarded as an extremely promising short-to-midterm solution for transportation needs.

Many types of hybrid transmission have been developed by the major automotive manufacturers in recent decades. Honda developed its two-motor hybrid system [1]. The system was installed in the 2014 Honda Accord and achieved a fuel consumption of 46 mpg in the charge-sustaining mode and 115 mpg equivalent in the charge-depleting mode. Mitsubishi also proposed a similar system and used in Mitsubishi Outlander PHEV with one more independent electric motor added to the rear wheels [2], making it a four-wheel drive system.

Toyota is one of the leading manufacturers of passenger hybrid vehicles, with the Prius being probably the most well-known. The Prius is based on the Hybrid Synergy Drive (HSD) [3], applying a PGT to provide more flexibility in maintaining the power sources in their respective high-efficiency regions. Ford developed a similar hybrid system [4], but the layout is quite different.

An increasing number of manufacturers now use CVT to improve the fuel efficiency of their hybrid vehicles by maintaining the power sources in their efficient working ranges. General Motors and Nissan's systems [5, 6] are the typical examples of hybrid CVTs. However, as for the other designs, vehicle reversing is possible only in the EV driving mode. Most of the hybrid transmission concepts were developed by experience or modification of the existing designs. Thus, there is a requirement for a more systematic design procedure for hybrid transmissions in order to ensure that the optimum design is obtained.

Paper Received October, 2019. Revised November, 2019. Accepted January, 2020. Author for Correspondence: Chun-Yao Yeh

* Associate Professor, Department of Mechanical Engineering, National Pintung University of Science and Technology, Pingtung, Taiwan 91207, ROC.

** Graduate Student, Department of Mechanical Engineering, National Pintung University of Science and Technology, Pingtung, Taiwan 91207, ROC.

CONCEPTUAL DESIGN

A systematical design procedure is proposed as shown in Fig. 1, which is based on the extension of creative mechanism design methodology [7] and Ngo’s design procedure of configuration synthesis for hybrid transmissions [8].

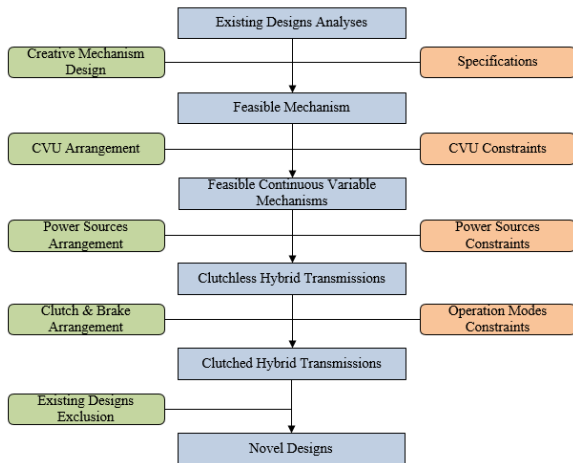


Fig. 1. Design procedure for hybrid CVTs

Based on the design procedure, novel hybrid CVTs can be synthesized by the following six steps:

Step 1. Existing designs analyses

Existing hybrid transmission designs are identified in the literature or patents, where each design is based on a CVT and offers the following operation modes: EV, engine alone, combined power, split power, regenerative braking, stationary charging, and mechanical reverse driving. Each design is analyzed in terms of its components, configuration and reverse driving mechanism. In this paper, Abe’s system [9] is selected as the existing design because a forward/reverse travel switching mechanism, PGT, is disposed between the input shaft and CVU, as shown in Fig. 2. It also has an engine (E), a generator (G), and a motor (M) as the power sources. By different engaging conditions of the clutch and brake, numerous operation modes are achieved.

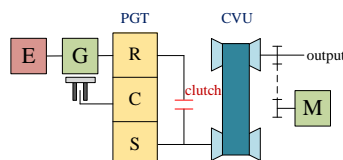


Fig. 2. Abe’s hybrid system

Step 2. Feasible mechanisms

The methodology of creative mechanism design [7] is applied to generate feasible mechanisms. In particular, the topological structures of the existing

designs are identified and the corresponding atlas of generalized chains obtained using a number synthesis algorithm [10]. The types of members and joints in each generalized chain are assigned using a process of specialization to obtain the atlas of feasible specialized chains. Finally, the feasible specialized chains are converted into corresponding schematic diagrams of feasible mechanisms. Finally, a reverse process of generalization graphically called particularization is applied. The feasible specialized chains are converted into the corresponding schematic diagrams of feasible mechanisms, as shown in Fig. 3.

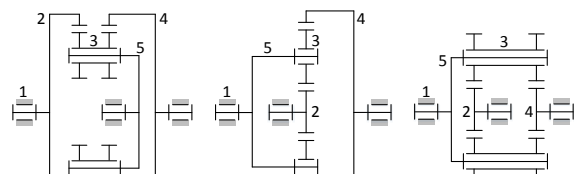


Fig. 3. Feasible mechanisms

Step 3. Feasible continuous variable mechanisms

Having obtained all the feasible mechanisms via the creative mechanism design methodology described above, the next step is to arrange the CVT. Fig. 4 shows all the feasible continuous variable mechanisms obtained subject to the following design constraints.

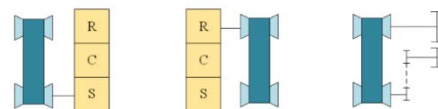


Fig. 4. Feasible continuous variable mechanisms

Step 4. Feasible continuous variable mechanisms

Once the feasible continuous variable mechanisms have been synthesized, a power arrangement process [8] is applied to assign the inputs and output to the synthesized mechanisms and obtain the corresponding atlas of clutchless hybrid CVTs.

Step 5. Feasible continuous variable mechanisms

Based on a clutch and brake arrangement technique, clutches and brakes are added to each clutchless hybrid transmission to have desired operation modes. And, the atlas of clutched hybrid CVTs can be obtained with the following requirements:

Step 6. Novel hybrid CVTs:

Finally, all the novel hybrid CVTs are generated by excluding the existing designs from the atlas of clutched hybrid CVTs. As a result, 21 novel hybrid CVTs are generalized, as shown in Fig. 5.

Every configuration has its own features with different pros and cons. In this paper, the design in Fig. 5(r) is selected for further analysis. This novel design can perform 11 operation modes as shown in Fig. 6. Six of them are forward modes, three of them are

reverse driving modes, and the other two are regenerative braking mode and stationary charging mode. Every operation mode is achieved by engaging different combination of the clutching conditions, as listed in Table 1.

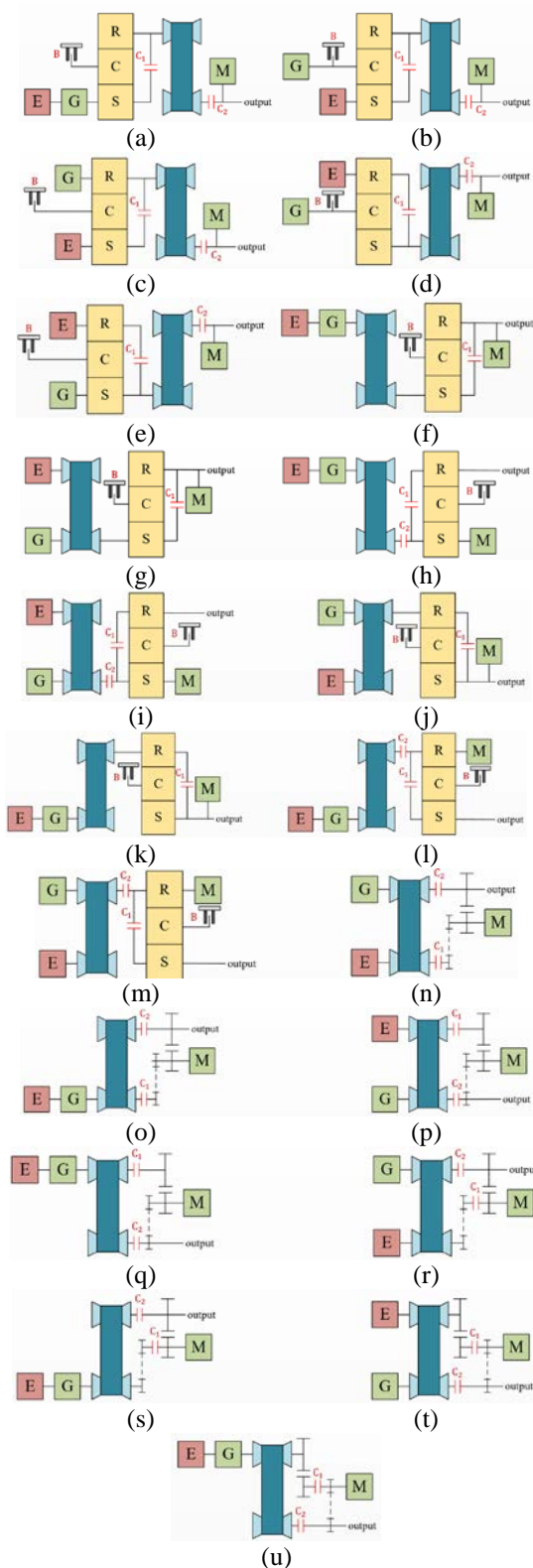


Fig. 5. Novel hybrid CVTs

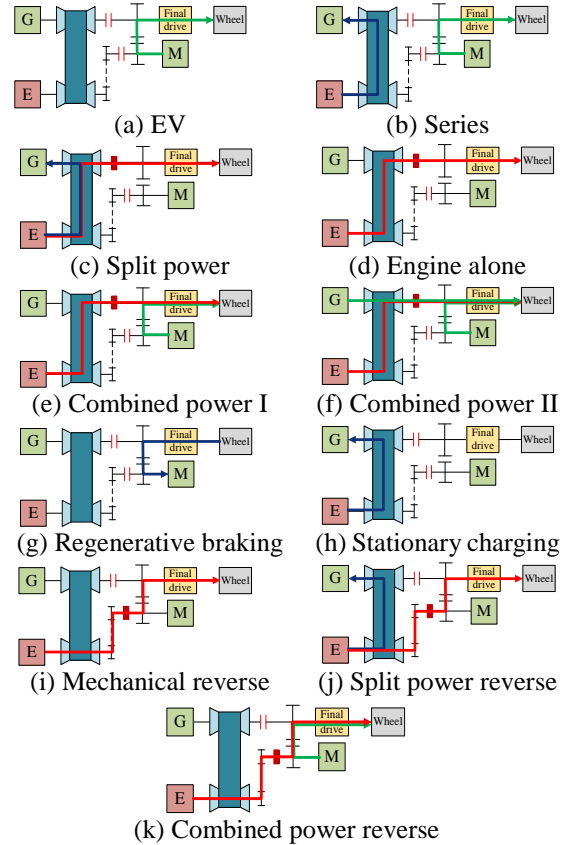


Fig. 6. Power flow of different operation modes

Table 1. Operation modes of proposed novel design

No.	Operating modes	Clutched	
		C ₁	C ₂
1	EV		
2	Series		
3	Split power		X
4	Engine alone		X
5	Combined power I		X
6	Combined power II		X
7	Regenerative braking		
8	Stationary charging		
9	Mechanical reverse	X	
10	Split power reverse	X	
11	Combined power reverse	X	

Modeling

In order to test the feasibility of the proposed novel design, vehicle dynamic, power source, transmission, and battery models are established for vehicle performance analysis and fuel economy simulation.

Vehicle dynamic model

When the vehicle is moving at a velocity v and up a slope of angle, the power sources provide traction force to overcome the resistance, including aerodynamic resistance, rolling resistance, and grade

resistance. These forces can be describes as:

$$F_{ar} = 0.5\rho C_d A_f v^2 \quad (1)$$

$$F_{rr} = C_{rr} mg \cos \theta \quad (2)$$

$$F_{gr} = mg \sin \theta \quad (3)$$

The vehicle speed is calculated using the equation of motion given by:

$$F_t = F_{ar} + F_{rr} + F_{gr} + m \frac{dv}{dt} \quad (4)$$

Power source models

Power sources are selected based on the evaluation of performance requirements. In this study, the technical data of the power sources is obtained from the software ADVISOR [11], as listed in Table 2.

Table 2. Specifications of the power sources

	Engine	Motor	Generator
Model	Saturn 1.9 L	Westinghouse	Prius_JPN
Max. torque	165 N-m	271 N-m	55 N-m
Max. power	95 kW	75 kW	15 kW
Max. speed	6,000 rpm	10,000 rpm	5,500 rpm
Max. eff.	0.34	0.90	0.84

Transmission model

For the optimization of fuel consumption and simulation purposes, the transmission model of this novel system must be built. The kinematic and dynamic characteristics of forward operation modes can be described as follows:

$$\omega_w = \frac{\omega_M}{i_g i_f} = \frac{\omega_E}{i_{cvt} i_f} = \frac{\omega_G}{i_f} \quad (5)$$

$$T_w = (T_E i_{cvt} \eta_{cvt} + T_M i_g \eta_g + T_G) i_f \eta_f \quad (6)$$

For reverse driving modes, the kinematic and dynamic characteristics are presented as:

$$\omega_w = \frac{\omega_M}{i_g i_f} = \frac{\omega_E}{i_c i_g i_f} \quad (7)$$

$$T_w = (T_E i_c \eta_c + T_M) i_g \eta_g i_f \eta_f \quad (8)$$

Battery model

In this paper, a valve-regulated lead-acid battery type is chosen. Its model is called Hawker Genesis [12]. In the battery pack, 26 Amp-h cells are connected in series, and there are totally 16 modules.

To evaluate the performance of the battery, a common technique is to calculate the state of charge by the following equation [13]:

$$SOC = SOC_i - \frac{\int_{t_i}^t I_b(\tau) d\tau}{C_{max}} \quad (9)$$

$$I_b = \frac{V_{oc} - \sqrt{V_{oc}^2 - 4RP_b}}{2R} \quad (10)$$

It is positive when the battery is discharging, negative when charging. And, P_b is calculated as:

$$P_b = T_M \omega_M + T_G \omega_G \quad (11)$$

Vehicle Performance

The performance of vehicle powertrains is generally evaluated in terms of the maximum vehicle speed, the acceleration time and the gradeability. In evaluating the performance of the hybrid CVT transmission system proposed in this research, the parameters used in the proposed novel system shown in Table 3.

Table 3. Parameters used in proposed novel system

Parameter	Value
Vehicle mass	1850 kg
Wheel radius	0.3262 m
Drag coefficient	0.335
Rolling coefficient	0.02
Frontal area	2.15 m ²
Air density	1.21 kg/m ³
Gravitational acceleration	9.81 m/s ²
CVT ratio	0.443~2.416
Gear ratio	1.1
Chain drive ratio	3.5
Final drive ratio	5.36
CVT efficiency	0.85
Gear efficiency	0.98
Final drive efficiency	0.95
Chain drive efficiency	0.95
Chain drive ratio	3.5

Top speed

The maximum vehicle speed is defined as the constant cruising speed that the vehicle can maintain with all the power sources engaged and providing full power. Under such a condition, the tractive effort and total resistance are in equilibrium, i.e.,

$$\frac{T_p i_t \eta_t}{r} = \frac{1}{2} \rho C_d A_f v^2 + C_{rr} mg \cos \theta + mg \sin \theta \quad (12)$$

The intersection points of the force curves with the total resistance curve represent the force equilibrium condition. In other words, the intersection points correspond to the velocity beyond which the vehicle speed cannot be further increased. With all the power sources driving the vehicle, the top speed is 226 km/h.

Acceleration time

The acceleration rate is one of the most important measures of a vehicle’s performance, and is defined as the time required for the vehicle to move from a stationary position to a certain high speed on level ground. In accordance with Newton’s second law, the acceleration of the vehicle can be calculated as:

$$a = \frac{dv}{dt} = \frac{F_t - F_R}{m} \quad (13)$$

Although the acceleration varies with the vehicle speed, it can be regarded as a constant value under the assumption of a sufficiently small change in the vehicle speed (Δv). Therefore, the time required to achieve a small increase in the vehicle speed can be approximated as:

$$t(i) = \frac{\Delta v}{a(i)} \quad (14)$$

Finally, the acceleration time to accelerate the vehicle from zero speed to 100 km/h is obtained by calculating the summation of all the little time. The acceleration time converges to a value of 7.1439 seconds given an incremental velocity of 0.001 km/h.

Gradeability

Gradeability is defined as the grade a vehicle can ascend maintaining a certain speed. Basically, the gradeability is represented as a percentage, where this percentage represents the inclination angle in accordance with.

$$G = \tan \theta \quad (15)$$

Graphical method is applied to analyze the gradeability of the vehicle as shown in Fig. 7. By adding the gradeability curves for the vehicle, i.e., the variation of the traction force required to maintain a certain vehicle velocity for different inclination angles, it is seen that the maximum gradeability is equal to 51.16 %, and is obtained in the combined power II operation mode.

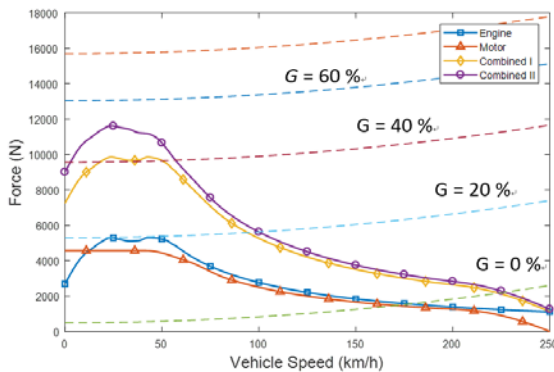


Fig. 7. Gradeability analysis

Simulation Structure

Fig. 8 shows the simulation structure of proposed simulator. Giving a driving cycle, simulation results are obtained for the ideal operating points of the individual power sources, the battery SOC, the CVT ratio, the shift process, and the fuel consumption. The simulation structure comprises four main components, as described in the following.

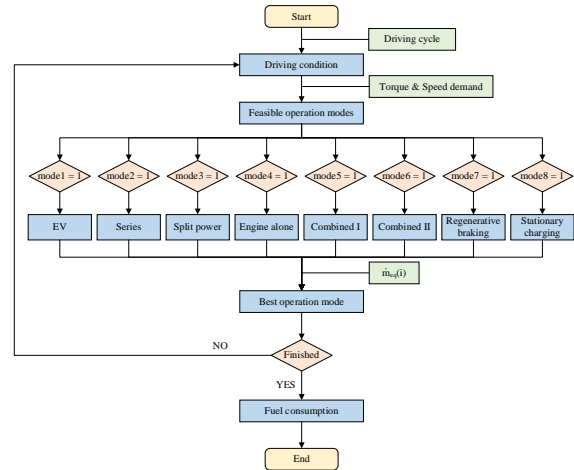


Fig. 8. Simulation structure

Part 1: Driving condition

A driving cycle is basically a series of data points showing the changes in the vehicle speed over time. Having selected a driving cycle, the required traction force at each time step is calculated based on Equation (4), with a zero slope. The corresponding torque demand (T_d) and speed demand (ω_d) on the wheels are then derived respectively as:

$$T_d = F_t \times r \quad (16)$$

$$\omega_d = \frac{v}{r} \quad (17)$$

Part 2: Feasible operation modes

The present research proposes the rule-based control strategy [15] shown in Fig. 9. As shown, the control strategy identifies the most feasible operation mode at every time step based on a joint consideration of the torque demand, the starting condition, the shifting smoothness, the capabilities of the power sources, and the SOC of the battery. Notably, the reverse driving modes are not considered in the control strategy since neither of the two driving cycles used in the present simulations involve the vehicle traveling in the reverse direction. If a particular operation mode is feasible, its switch is set to be “ON”. For example, mode1=1 when the EV mode is feasible.

Part 3: Best operation mode

Once a switch is set to be “ON”, the corresponding subroutine is launched to calculate the

torque and speed that the power sources need to supply. In order to minimize the fuel consumption, the equivalent consumption minimization (ECSM) [16] is applied. The objective function, equivalent fuel consumption, is:

$$f = \dot{m}_E + \frac{SC_E P_M}{\eta_M} - SC_E P_G \eta_G \quad (18)$$

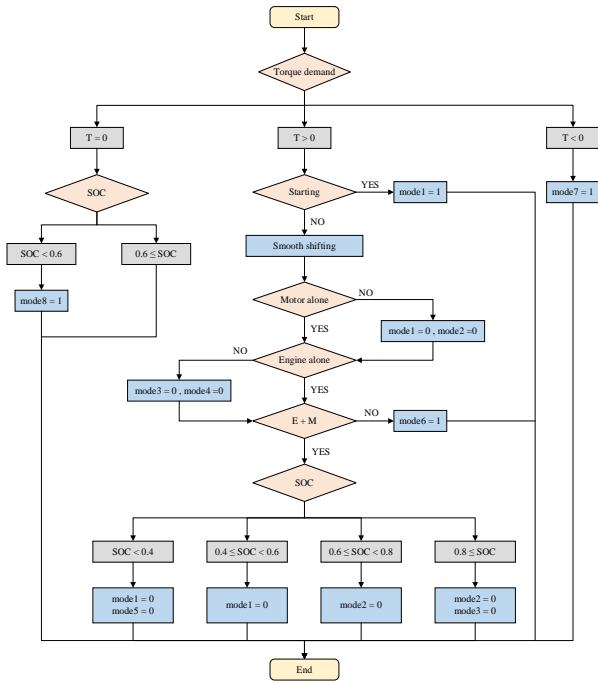


Fig. 9. Control strategy

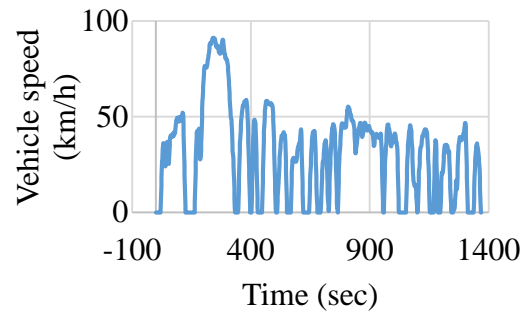
Part 4: Fuel consumption

The fuel consumption of the vehicle is evaluated by determining the total amount of fuel used by the vehicle in traveling the distance associated with the selected driving cycle. The total fuel consumption is determined by deriving the equivalent fuel consumption at each of the operating points in the simulation and then integrating the results over all the operating points in the cycle. Similarly, the distance traveled by the vehicle during the driving cycle is evaluated as the area under the corresponding velocity-time curve. The average fuel consumption is then obtained simply by dividing the total consumed fuel by the total distance.

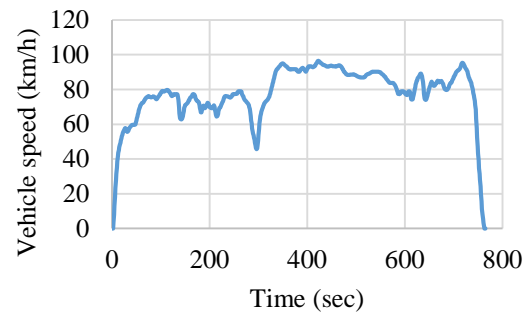
Simulation Result

Given the proposed control strategy and the fuel consumption analysis, simulations were performed to evaluate the operating points in the power source efficiency maps, the CVT ratio data, the battery SOC, and the historical operation mode for each of the two EPA driving cycles as shown in Fig. 10.

Fig. 11 shows the simulated operating points, red circles, in the engine efficiency map during the urban



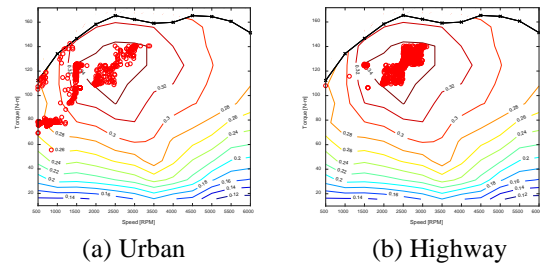
(a) Urban



(b) Highway

Fig. 10. Operating points in engine efficiency map

and highway cycles, respectively. In the urban cycle, the power demand is sometimes high and sometimes low, depending on the road conditions. Consequently, the operating points are widely scattered in the energy efficiency map and are not always located in the region of highest efficiency. For the highway cycle, the vehicle speed remains high most of the time. Consequently, the vehicle is driven mainly in the engine alone mode, and hence almost all of the operating points are located within the high-efficiency region of the efficiency map since the control strategy seeks to minimize the fuel consumption over the duration of the driving cycle.



(a) Urban

(b) Highway

Fig. 11. Operating points in engine efficiency map

Fig. 12 shows the operating points in the motor efficiency map during the two driving cycles. For the urban cycle, many operating points are associated with a negative torque due to the inherent “stop and go” nature of urban driving. Under such driving conditions, the controller frequently selects the regenerative

braking mode to scavenge energy to recharge the battery. Furthermore, since the engine works poorly at low vehicle speeds, the controller mainly selects the EV mode to drive the vehicle. Since the power demand is not high when the EV mode is used, none of the operating points are located in the high-efficiency region of the map. Under highway driving conditions, the vehicle travels at a high speed. However, the power demand is not as high as that when the vehicle is climbing or accelerating. Consequently, the motor is not required to support the engine under the combined power mode. Moreover, in contrast to the urban cycle, the vehicle does not stop during highway driving. Consequently, the motor is seldom required in the highway cycle, and hence the efficiency map contains relatively fewer operating points.

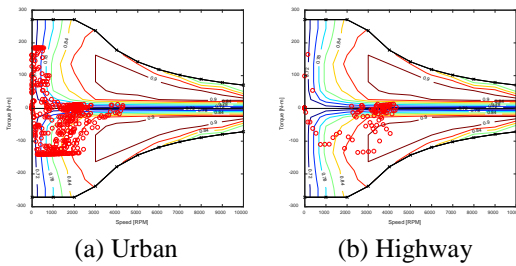


Fig. 12. Operating points in motor efficiency map

Fig. 13 shows the operating points in the generator efficiency map. For both driving cycles, all of the operating points are associated with a positive torque. In other words, combined power mode II is not used in either cycle. Operating points with a negative torque imply that the generator receives power from the engine. Thus, the results presented in Fig. 13 show that the split power mode is selected frequently in both driving cycles. In addition, compared to highway driving, the road conditions in urban driving vary more dramatically. Consequently, the operating points in Fig. 13 (a) are more widely scattered than those in Fig. 13 (b).

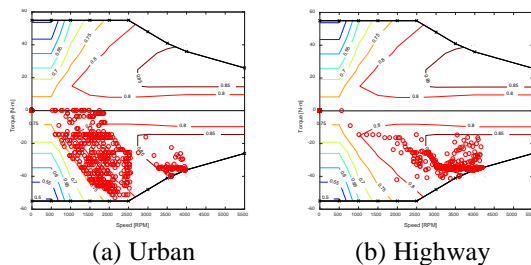


Fig. 13. Operating points in generator efficiency map

The CVT reduction ratio changes continuously over the driving cycle in accordance with changes in the instantaneous power demand. Fig. 14 shows the historical values of the CVT ratio in the simulated urban and highway cycles. For urban driving, the

vehicle speed changes frequently in response to changing driving conditions. Consequently, the CVT ratio varies widely over the duration of the driving cycle. However, in highway driving, the vehicle speed remains relatively constant and the vehicle never stops. As a result, the CVT ratio is maintained in the range of 0.5-1 for virtually the entire driving cycle.

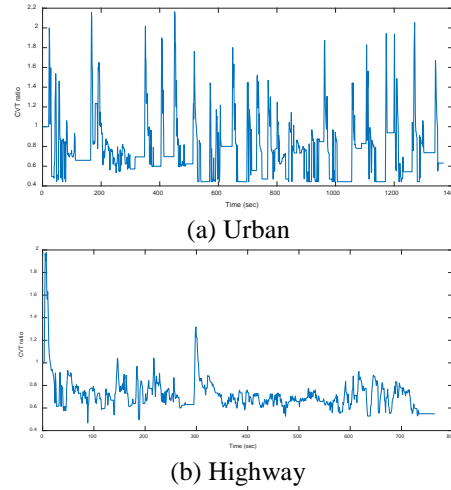


Fig. 14. Historical data of CVT ratio

The simulations assumed an initial battery SOC of 0.6. In other words, the battery lacked power initially. However, the proposed control strategy uses the engine to drive the generator and generate electricity to charge the battery whenever it is feasible (and necessary) to do so. Consequently, as shown in Fig. 15, the SOC increases with time, irrespective of the driving cycle (urban or highway). Notably, the SOC approaches a final value of approximately 0.625 in both cycles. However, the required charging time is longer under urban driving conditions than under highway driving. Furthermore, the vehicle operates mainly in the EV mode under urban driving, and hence the motor draws heavily on the battery power to drive the vehicle. Consequently, the rate at which the SOC increases is reduced.

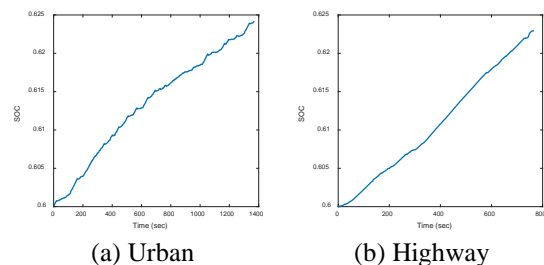


Fig. 15. Historical data of SOC

The proposed novel design consumes 45 and 36 miles per gallon in urban and highway respectively, which is very competitive to the existing HEVs developed by some well-known automakers as listed

in Table 4. The key point that Toyota Prius and Hyundai Ioniq consume less fuel is their lightness. The mass of the proposed novel design is larger than the other vehicles, but it still consumes less fuel consumption than Ford Fusion and Chevrolet Volt in urban.

Table 4. Fuel economy of the existing HEVs

HEVs	Mass (kg)	Urban (MPG)	Highway (MPG)
Toyota Prius (2017)	1397	54	50
Hyundai Ioniq (2017)	1439	55	54
Honda Accord (2017)	1580	49	47
Ford Fusion (2017)	1556	43	41
Chevrolet Volt (2017)	1607	43	42

Fig. 16 compares the simulated vehicle velocity with the target velocity during both driving cycles. The simulated vehicle speed is obtained by applying the kinematic model with the historical data of operating points and CVT ratios. It is observed that a good fit exists between the two velocity profiles. Hence, the validity of the simulation results is confirmed.

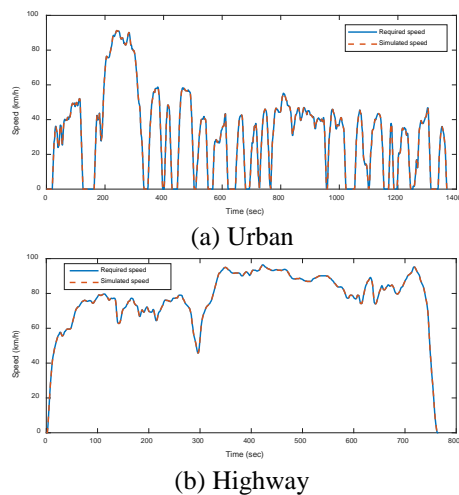


Fig. 16. Simulation verifications

Conclusions

The transmission system is a key component of HEVs and has a critical effect on the vehicle performance. Numerous designs have been presented for HEV transmissions. However, these designs are generally based on the designers' personal experience and preferences. Hence, there is a danger that the

optimal HEV design may be overlooked. Accordingly, this paper has presented a systematic design methodology for CVT-based HEV transmission systems encompassing the conceptual design, the detailed design, systems analysis, and computer simulation and verification.

As the result, 21 novel hybrid CVTs are synthesized, 13 of them using PGT as reverse mechanisms and 8 of them applying chain drives. Assuming the installation of the proposed design in a vehicle with known specifications, it is shown that the transmission system makes possible a maximum vehicle speed of 226 km/h, a 0 ~100 km/h acceleration time of 7.1439 seconds, and a gradeability of 51.16 %. A simulation model is developed to investigate the fuel efficiency performance of the proposed design. With a ruled-based control strategy and optimization for fuel consumption, it is shown that the simulated vehicle with the proposed hybrid CVT achieves a fuel consumption of 45 mpg under urban driving cycles and 36 mpg under highway driving conditions.

ACKNOWLEDGMENT

This work is mainly funded through the project (MOST No. 104-2221-E-006- 059-MY3) by the Ministry of Science and Technology (Taiwan). The authors would like to thank for their supports with the greatest appreciations.

REFERENCES

Honda, K. and Yumoto, T., "Driving apparatus for hybrid vehicle," U.S. Patent No. 8,430,190 (2013).

Nissato, Y., "Clutch control device of hybrid vehicle," U.S. Patent No. 8,608,616 (2013).

Nagano, S., Morisawa, K. Matsui, H., and Ibaraki, R., "Hybrid drive system wherein planetary gear mechanism is disposed radially inwardly of stator coil of motor/generator," U.S. Patent No. 6,155,364 (2000).

Kraska, M. P. and DeMurry, T. L., "Torque reversal reduction strategy for a hybrid vehicle," U.S. Patent No. 6,600,980 (2003).

Tamai, G. and Hoang, T. T., "CVT hybrid powertrain fueling and engine stop-start control method," U.S. Patent No. 6,945,905 (2005).

Matsuo, I., Nakazawa, S., Maeda, H., and Inada, E., "Development of a high-performance hybrid propulsion system incorporating a CVT," SAE Technical Paper No. 2000-01-0992 (2000).

Yan, H. S., "A methodology for creative mechanism design," Mechanism and Machine Theory, 27.3: 235-242 (1992).

Ngo, H. T. and Yan, H. S., "Configuration synthesis of parallel hybrid transmissions," Mechanism and Machine Theory, 97: 51-71 (2016).

Ngo, H. T. and Yan, H. S., "Novel Configurations for Hybrid Transmissions Using a Simple

- Planetary Gear Train,” ASME Trans., Journal of Mechanisms and Robotics, 8.2: 021020 (2016).
- Abe, N., Kimura, H., Fuchino, M., and Hasebe, T., “Hybrid vehicle,” U.S. Patent No. 7,506,710 (2009).
- Yan, H. S. and Chiu Y. T., “An improved algorithm for the construction of generalized kinematic chains,” Mechanism and Machine Theory, 78: 229-247 (2014).
- Markel, T., Brooker, A., Hendricks, T., Johnson, V., Kelly, K., Kramer, B., and Wipke, K., “ADVISOR: a systems analysis tool for advanced vehicle modeling,” Journal of Power Sources, 110.2: 255-266 (2002).
- Brooker, A., Haraldsson, K., Hendricks, T., Johnson, V., Kelly, K., Kramer, B., and Zolot, M., “Advisor Documentation,” National Renewable Energy Laboratory, 4: 76 (2002).
- Piller, S., Perrin, M., and Jossen, A., “Methods for state-of-charge determination and their applications,” Journal of Power Sources, 96(1), 113-120 (2001).
- Van Mierlo, J., Van den Bossche, P., and Maggetto, G., “Models of energy sources for EV and HEV: fuel cells, batteries, ultracapacitors, flywheels and engine-generators,” Journal of Power Sources, 128.1: 76-89 (2004).
- Chen, L., Zhu, F., Zhang, M., Huo, Y., Yin, C., and Peng, H., “Design and analysis of an electrical variable transmission for a series-parallel hybrid electric vehicle,” IEEE Trans. on Vehicular Technology, 60.5: 2354-2363 (2011).
- Paganelli, G., Guezennec, Y., and Rizzoni, G., “Optimizing control strategy for hybrid fuel cell vehicle,” SAE Technical Paper No. 2002-01-0102 (2002).
- g the gravitational acceleration constant
- ω_i the rotational speeds of the element i
- T_i the torque of the element i
- P_i the power of the element i
- i_i the reduction ratio of the element i
- η_i the efficiency of the element i
- SOC the state of charge
- V_{oc} the open-circuit voltage
- R the circuit resistance
- I_b the current
- P_b the battery power
- a the acceleration
- t_a the acceleration time
- G the gradeability
- f the equivalent fuel consumption
- \dot{m}_E the fuel mass flow rate
- SC_E the equivalent fuel consumption conversion factor

NOMENCLATURE

- θ the slope of road
- F_t the traction force
- F_{ar} the aerodynamic resistance
- F_{rr} the rolling resistance
- F_{gr} the grade resistance
- ρ the air density
- C_d the aerodynamic drag coefficient
- A_f the frontal area
- C_{rr} the rolling coefficient
- m the vehicle mass

含引擎驅動倒檔混合動力 無段變速系統之創新設計

葉駿耀 顏鴻森

國立成功大學機械工程學系

摘要

隨著全球環保意識抬頭以及國際法規對於傳統引擎車的限制，汽車產業致力於發展綠能車輛，然而現有純電動車存在許多電池技術及便利性問題，使得普遍消費者較無法接受。因此近年來，混合動力車迅速的發展，其繼承了引擎車及電動車的優點，不但行駛時有平穩的動力和良好的加速性能，更有效降低油耗及空氣污染。

混合傳動系統為耦合動力不可或缺的一環，本論文旨在發展一套系統化的設計流程，基於創意性機構設計方法之擴展，系統化地整合出所有可行的並聯式傳動系統，並透過分析及模擬驗證新型設計之可行性。首先，建立車輛及電池之模型，根據性能需求選擇適當的動力源。接著採用本論文所提出之設計方法，依據設計需求與限制，並以現有 Punch VT2 為基礎，產出所有可行混合動力無段變速系統之新型構想，計合成出 21 個新型設計，其中 13 個應用行星齒輪機構，8 個應用鏈輪及齒輪的組合以達成引擎倒檔的特殊需求。由概念評估，其中一個新型概念被選出來進行細部設計及分析，將此傳動系統安裝置一台已知規格之車輛中，其車輛性能為：最大車速 226 km/h、從 0 至 100 km/h 之加速時間 7.1439 秒、爬坡度 51.16 %。

最後，本研究設計出一套針對此新型混合動力車的模擬器以進行模擬油耗的分析，亦建立了一套控制邏輯，使車輛在行駛中自動換檔，在不同路況下選擇最適當的檔位。為減少油耗，本研究考量動力源特性、無段變速之減速比與連續性、檔位切換的順暢性、電池電量等各種限制下，針對充電效率及各操作模式的油耗進行最佳化。在 EPA 標準之測試規格下，此新型混合動力車在市區及高速公路的油耗分別為 45 和 36 MPG，與其他現有混合動力車相比，具有相當大的競爭力。